

Impact of triplet absorption and triplet-singlet annihilation on the dynamics of optically pumped organic solid-state lasers

M. Lehnhardt,¹ T. Riedl,^{2,3,*} T. Weimann,¹ and W. Kowalsky³¹Physikalisch-Technische Bundesanstalt, Bundesallee 100, 38116 Braunschweig, Germany²Institute of Electronic Devices, University of Wuppertal, Rainer-Gruenter-Strasse 21, 42119 Wuppertal, Germany³Institut für Hochfrequenztechnik, Technische Universität Braunschweig, Schleinitzstrasse 22, 38106 Braunschweig, Germany

(Received 16 February 2010; published 27 April 2010)

We study the dynamics of a diode pumped organic semiconductor laser based on the polymer-polymer guest-host system F8BT and MEH-PPV. Regardless of the duration of the pump pulse, lasing persists for only a few nanoseconds. In two separate experiments we study in detail the contribution of triplet-singlet annihilation and triplet state absorption. On this basis we were able to model the laser dynamics. As a result, we show that depending on the supplied energy density of the pumping source, triplet-singlet annihilation or triplet state absorption play the prevalent role.

DOI: [10.1103/PhysRevB.81.165206](https://doi.org/10.1103/PhysRevB.81.165206)

PACS number(s): 78.66.Qn, 42.70.Jk, 78.45.+h

I. INTRODUCTION

In recent years, organic solid-state lasers (OSL) seeded the prospect for cost effective and widely tunable laser sources.¹ Especially, OSL pumped by an inorganic laser diode² or even a light emitting diode³ have recently received considerable attention. As is known from liquid based dye lasers, continuous-wave operation is usually hindered by a pileup of triplet excitons.⁴ For organic solid-state lasers the highest repetition rates published were 5 MHz.⁵ As opposed to liquid based systems, a sound understanding of the dynamics in OSL has not been achieved. Especially, the contribution of triplet-singlet annihilation (TSA) and triplet state absorption (TA) is still under debate. Recently, Giebink and Forrest⁶ have studied the laser dynamics in an organic distributed feedback (DFB) laser and have attributed their findings exclusively to TSA without taking TA into account. Reufer *et al.*⁷ studied the triplet density in an OSL but did not explain the observed increase in the triplet density above lasing threshold. In this paper, we study the dynamics of an OSL based on a polymer-polymer guest-host gain medium of poly[(9,9-di-n-octylfluorenyl-2,7-diyl)-alt-(benzo[2,1,3]thiadiazol-4,8-diyl)] (F8BT) and poly[2-methoxy-5-(2-ethylhexyloxy)-1,4-phenylenevinylene (MEH-PPV)]. We find that lasing emission persists only for the first nanoseconds of the excitation pulse. We experimentally separate the impact of both TSA and TA. Thereby, we can model the laser dynamics and show that both TSA and TA play an important role, depending on the supplied energy density.

II. EXPERIMENTAL DETAILS

For the OSLs we employ second-order DFB resonators with a 180-nm-thick gain medium (F8BT/MEH-PPV 16 wt %) on a silicon dioxide substrate. As a source for optical pumping we used a Q-switched, frequency-tripled, diode pumped solid-state (DPSS) laser emitting at $\lambda = 355$ nm. The pulse width and repetition rate were 700 ps and 2 kHz, respectively. The second pumping source used in this research is an InGaN based laser diode ($\lambda = 445$ nm)

provided by Nichia Chemical (NBD7112). The laser diode was driven with a variable pulse width and a repetition rate of 2 kHz. For diode pumped OSL, the multimode output of the diode is collimated and focused to a spot of $170 \times 290 \mu\text{m}^2$. For time-resolved measurements we used a streak camera. In this measurement the OSL was excited by the blue laser diode with a pulse length of 70 ns and pulse an pulse energy of 266 nJ, which is approximately 33 nJ above the lasing threshold. During all optical measurements, the samples were mounted in a nitrogen purged sample chamber.

The gain spectrum was measured with the variable stripe length method.^{8,9} Due to the very short pulse length of the DPSS pump laser the pileup of triplets can be neglected, as we show in our model, detailed in the following. As can be seen from the gain measurement this system provides a large differential gain (gain vs pumping intensity) and a broad gain spectrum even at low excitation densities (Fig. 1 inset). As a result the emission wavelength of the organic lasers could be tuned between 592 and 690 nm upon pumping with the DPSS laser depending on the periodicity of the Bragg grating with a minimum laser threshold of approximately $1.4 \mu\text{J}/\text{cm}^2$ at 638 nm. The line scan of the time-resolved

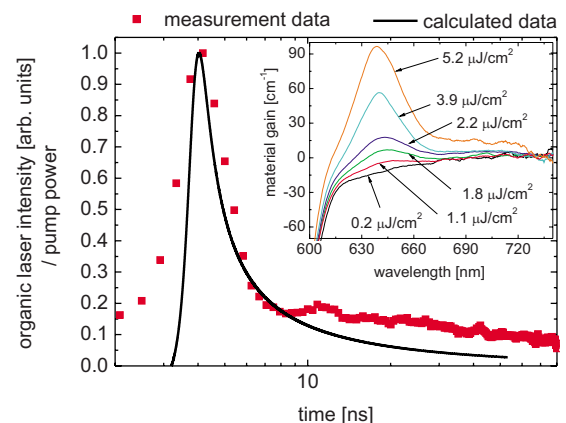


FIG. 1. (Color online) Time-resolved image of the OSL emission and simulated data from our model (Fig. 4). Inset: optical gain spectrum in F8BT/MEH-PPV (16 wt %) at low excitation densities.

measurement (Fig. 1) at 638 nm, of the OSL output intensity divided by the pump power of the blue laser diode, shows that lasing action persists only for the first 3 ns of the excitation pulse.

A common explanation for this observation is that during the excitation pulse long-lived triplet excitons were formed by intersystem crossing (ISC) of the optically generated singlet excitons in the gain material and finally cause termination of the lasing process.⁴ For our solid-state waveguide structure, it is essential to distinguish between TA and TSA. To this end, we designed two independent pump-probelike experiments. In both experiments triplet excitons are generated by ISC of singlets excited by a pump pulse of the laser diode. A probe pulse from the DPSS laser trails the laser diode pulse with a time delay of 200 ns. Both experiments were not done in laser structures but on a silicon dioxide substrate (without resonator grating) and on a native oxide silicon substrate, respectively. Considering the highest occupied molecular orbital/lowest unoccupied molecular orbital levels in our guest-host system it can be ruled out that a donor/acceptor system is formed.^{10,11} It is worth to note that during optical excitation aside from singlet excitons and long-lived triplets, polaron pairs can be generated in PPV.^{12–16} Polaron pairs in PPV were reported to have an absorption peak between 1.4 and 1.5 eV,^{12,14,15} which is spectrally very similar to the triplet absorption peak centered around 1.45 eV.¹⁷ Polaron pairs decay times were presented up to milliseconds.^{14–19} Although the influence of polaron pairs in our experiments cannot be excluded completely, we will show that triplet states are predominantly responsible for the observed effects in the following experiments. This will be verified by carrying out control experiments under oxygen and nitrogen atmosphere, which will be presented later. On contrary, in the optical gain measurements presented above, polaron pairs have some impact. Due to their very fast generation time within approximately 100 fs (Ref. 13) they appear in a significant quantity by pumping with the DPSS laser and will reduce the material gain. In our model the influence of polaron pairs is therefore included by the gain coefficient, determined from the gain measurement (Fig. 1 inset). Initially, we studied the TA in the pristine host, the pristine guest, and the host/guest system, respectively. The absorption was measured using a waveguide structure consisting of a 180-nm-thick F8BT/MEH-PPV layer on top of a silicon substrate with a 2- μm -thick SiO_2 layer. TSA can be excluded by spatially separating the pump and the probe pulse on the sample by 0.1 mm [Fig. 2(a)]. Exciton diffusion from the pump area to the probe pulse area is not possible due to the low diffusion length of 5–8 nm.^{20,21} The probe pulse generates light which propagates through the waveguide toward the sample edge and has to pass the region of the waveguide where triplets have been generated by the pump pulse. A highly sensitive measurement is possible because of a long interaction path length (~ 0.5 mm) of the probe photons with potentially elevated waveguide losses due to TA.

Figure 2(b) shows the reduction in the probe pulse induced light intensity emitted from the sample edge for increasing energy density and varying duration of the pump pulse. Here, the organic guest-host system was studied. Due

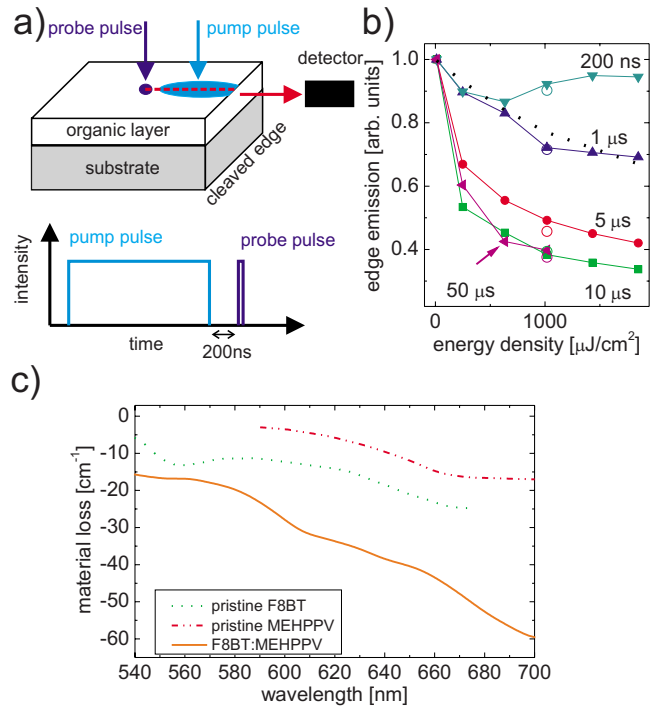


FIG. 2. (Color online) (a) Setup for TA measurement. (b) Decrease in edge emission at varied pump pulse duration and energy density for F8BT/MEH-PPV. Fitted values for the saturation over the pulse length (open circles) and an exemplary fit over the energy density (dotted line) for a pulse duration of 1 μs . (c) TA in pristine F8BT, pristine MEH-PPV, and F8BT/MEH-PPV.

to the dimensions of the waveguide only the first transversal electric mode can propagate. Photothermal or photorefractive effects, which would lead to a change in the refractive index, cannot lead to the propagation of higher modes in our waveguide. Only a slight change in the mode intensity overlap with the organic layer can be expected.²² Therefore the measured decay of edge emission up to 66% must be caused by an additional material absorption. A clear saturation behavior is found with increasing energy density and pump pulse length. Figure 2(c) shows the resulting absorption spectra (diode laser pulse: duration 10 μs and energy density 1020 $\mu\text{J}/\text{cm}^2$). The determined spectral characteristics are in good agreement with reported triplet absorption spectra,^{23,24} which showed a very broad absorption peaking around 800 nm and extending up to 550 nm. Hale *et al.*²⁵ showed that triplet-triplet annihilation (TTA) is a major decay mechanism for photoexcited triplet excitons. During the excitation time of the pump pulse a further loss mechanism for triplets is polaron-triplet annihilation (TPA).²⁶ The density of long-lived triplets increases during excitation and reaches orders of magnitude higher values than the polaron density. Because of this TPA is a minor effect in our experiment compared to TTA and is not taken into account in the following discussion. With the model we describe later in the paper we are able to fit the data of Fig. 2(b) using the TTA rate k_{tt} as fit parameter.

In the second experiment, TSA will be studied. Here, the pump and the probe pulse are focused on the same position of the sample. As opposed to the previous experiment, we

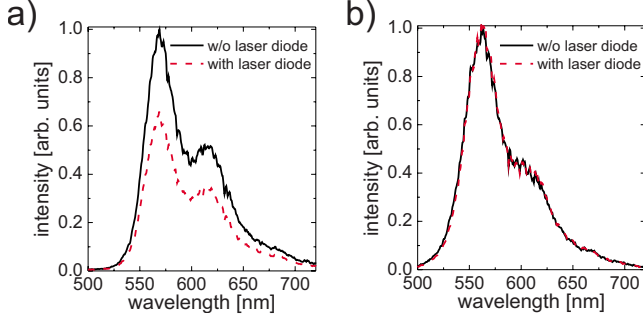


FIG. 3. (Color online) (a) Quenching of photoluminescence due to triplet states in nitrogen ambience and (b) in oxygen ambience.

used a sample consisting of a 180-nm-thick layer of F8BT/MEH-PPV on top of a silicon substrate with native oxide. Owing to the strong absorption of silicon in the spectral region of our experiment, the waveguide absorption is very high. Therefore, waveguided modes are efficiently suppressed and can be neglected. The photoluminescence (PL) as a result of the probe pulse is detected perpendicular to the sample surface with and without a previous pump pulse (which leads to triplet generation). The laser diode is focused with a spot size of $1.2 \times 2.5 \text{ mm}^2$ (pulse length $10 \text{ }\mu\text{s}$ and pulse energy $3.36 \text{ }\mu\text{J}$). The probe-laser spot is somewhat smaller ($1 \times 1 \text{ mm}^2$) aligned with the center of the laser diode spot. In view of the previously determined maximum TA for the host/guest system (at 638 nm) and a film thickness of 180 nm, a maximum relative decrease in the emitted photoluminescent intensity due to TA is expected to be less than 0.07%. On the contrary, Fig. 3(a) displays a substantial decay in the probe PL intensity of about 39% when triplet excitons have been generated by the diode laser pump pulse. This cannot be attributed to TA but rather to TSA. Owing to the Förster-type energy transfer in TSA, the spectral characteristics result from the overlap of the PL and the triplet absorption spectrum.^{27,28} To prove that triplet states are mainly responsible for the observed effects we repeated the PL quenching measurement again in oxygen ambient rather than in nitrogen. Triplet states are able to transfer their to oxygen which has been evidenced to be an sufficient triplet quencher.²⁹ This will dramatically decrease the triplet lifetime and therefore reduce the measured PL quenching effect.³⁰ The measurement results are shown in Fig. 3(b) with the same setup as above but in an test chamber purged with 99.9995% oxygen. In this case no PL quenching can be observed with a time delay of 200 ns. Subsequently, we repeated the experiment at the same sample position under nitrogen ambient. Here, the quenching of the PL is encountered again. This clearly shows that triplet excitons are the predominant origin of our observations discussed above.

III. RESULTS AND DISCUSSION

Due to the efficient Förster energy transfer from F8BT to MEH-PPV and the high doping concentration of 16 wt %, it is reasonable to expect that the majority of triplets is located on the guest molecules. In addition, we measured a triplet lifetime at room temperature in thin films of pristine F8BT

(1.8 μs), pristine MEH-PPV (4 μs), and for the host/guest system (138 μs) (will be published elsewhere). This surprisingly long lifetime in the host/guest system is similar to values observed for MEH-PPV in highly diluted benzene solution,²⁴ where self-quenching is insignificant. This strongly supports the model in which the triplet excitons are located on the MEH-PPV guest molecules. From the TA spectrum an assignment of the triplet excitons to guest or host is not obvious due to similar spectral absorption characteristics [Fig. 2(c)]. For a quantitative assessment of the laser dynamics we use the previous experiments to extract the TSA rate k_{st} and the TTA rate k_{tt} .

We have to consider the following reactions which take place in our system: $S_1 + T_1 \xrightarrow{k_{st}} T_1 + S_0$; $T_1 + \text{photon} \xrightarrow{\sigma_t} T_n$. Furthermore TTA and singlet-singlet annihilation (SSA) play a role at higher exciton densities. In case of TTA (SSA) two triplets (singlets) can react to one singlet or one triplet state, respectively. The ratio of generated singlet to triplet excitons is described by the parameter ξ which is assumed to be 0.25.³¹ Further details about this processes have been published by Gärtner *et al.*³² In order to express the dynamics of our OSL structure pumped by the laser diode we used the following three rate equations:^{6,32}

$$\frac{dn_s}{dt} = G - \frac{n_s}{\tau_s} - k_{st}n_s n_t - (2 - \xi)k_{ss}n_s^2 - k_{isc}n_s - n_s\sigma_g \frac{c}{n_{\text{eff}}} S, \quad (1)$$

$$\frac{dn_t}{dt} = n_s k_{isc} - \frac{n_t}{\tau_t} + (1 - \xi)k_{ss}n_s^2 - (1 + \xi)k_{tt}n_t^2, \quad (2)$$

$$\frac{dS}{dt} = (\Gamma n_s \sigma_g - \alpha_{\text{cav}} - n_t \sigma_t) \frac{c}{n_{\text{eff}}} S + \Gamma \beta_{\text{sp}} \frac{n_s}{\tau_s}. \quad (3)$$

Here the singlet density is described by n_s , the triplet density by n_t , and the photon density in the lasing mode by S . G is the generation rate of singlet excitons produced by the optical pump pulse. The effective refractive index n_{eff} and the transversal mode confinement factor Γ are both calculated by waveguide simulation while the spontaneous emission factor β_{sp} is assumed to be 10^{-46} . From the TA measurement shown in Fig. 2(c) and the calculated corresponding triplet density we derive a cross section σ_t of $5 \times 10^{-16} \text{ cm}^2$ at a wavelength of 638 nm, which is in reasonable agreement with values reported before ($2 \times 10^{-16} - 1.5 \times 10^{-15} \text{ cm}^2$).³³ The cavity loss, α_{cav} , is evaluated considering the lasing threshold and using the gain cross section $\sigma_g = 1 \times 10^{-15} \text{ cm}^2$, determined above (Fig. 1 inset). The term $n_t \sigma_t$ takes the increase in cavity loss due TA into account. In our host/guest system we measured a triplet lifetime of 138 μs at room temperature which can be considered as a lower limit for τ_t in our model. For the singlet lifetime, τ_s , we use a value of 200 ps as reported for MEH-PPV.³⁴ An intersystem crossing rate, k_{isc} , of $\approx 7 \times 10^6 \text{ s}^{-1}$ has been reported by several authors.^{24,26,35} With an SSA rate k_{ss} of less than $10^{-8} \text{ cm}^3/\text{s}$ (Ref. 32) this process is found to be negligible in our experiments. For the exact description of the dynamics of our polymer host/guest laser the rates for STA k_{st} and TTA k_{tt} are of

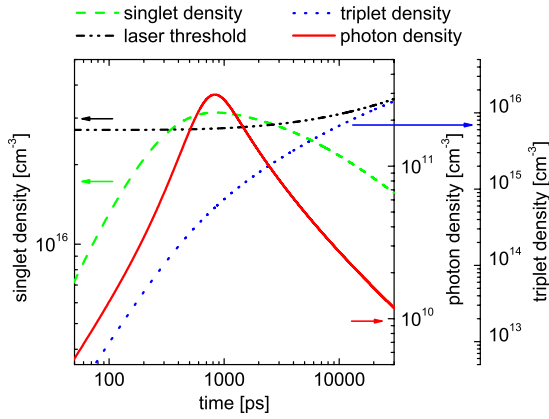


FIG. 4. (Color online) Simulation results of singlet, triplet, and photon density for the diode pumped OSL shown in Fig. 1.

paramount importance. Only very limited data for k_{st} (Refs. 27 and 36) and k_{tt} (Ref. 32) has been published. By fitting our model to the experimental data of the PL-quenching experiment and the TA measurement [Fig. 2(b)], both values can be determined. Best fit parameters are: $k_{st}=4 \times 10^{-7} \text{ cm}^3/\text{s}$ and $k_{tt}=1.5 \times 10^{-12} \text{ cm}^3/\text{s}$. With these values, the saturation of TA with increasing pump density and pump pulse length [Fig. 2(b)] as well as the results from the PL-quenching [Fig. 3(a)] experiments can be favorably simulated. While k_{tt} is in good agreement with reported data,³² k_{st} is substantially higher than previously published values^{27,36} for pristine materials. To our knowledge no TSA rates for host/guest systems have been published. It was shown that TSA is based on Förster energy transfer^{27,28} requiring a spectral overlap of the PL spectrum and the TA spectrum. As is obvious from Fig. 2(c), a substantial spectral overlap is found in our case.

On basis of our model and the data determined for k_{st} and k_{tt} , we are now able to fully describe the dynamics of our diode pumped laser as discussed in Fig. 1. Figure 4 shows the results of our calculation for the OSL. Initially, the singlet density is increasing very fast and the laser threshold is reached. This is accompanied by a dramatic increase in the photon density. Compared to this, triplet excitons are forming relatively slow by ISC. However, due to their long lifetime, triplet excitons accumulate over time. With an increasing density of triplets, the singlet density is reduced due to TSA. In addition, the piled-up triplets increase the laser threshold due to TA which results in a rise of the waveguide losses. Both, the increasing laser threshold and the decreasing singlet density, finally cause a termination of the laser action. The calculated photon density gives a duration of the laser output pulse of $\approx 3 \text{ ns}$. This is in excellent agreement with the measured laser-pulse duration of the diode pumped organic laser (Fig. 1). The discrepancy in the first few nanoseconds is caused by the not ideal square pulse of the excitation source, as assumed in our model. After termination of lasing the detected intensity is a little higher than calculated. Here, the spontaneous emission from organic gain material surrounding the not ideal laser spot is relevant.

The pulse duration of the organic laser output can be increased by increasing the optical pump power density (i.e.,

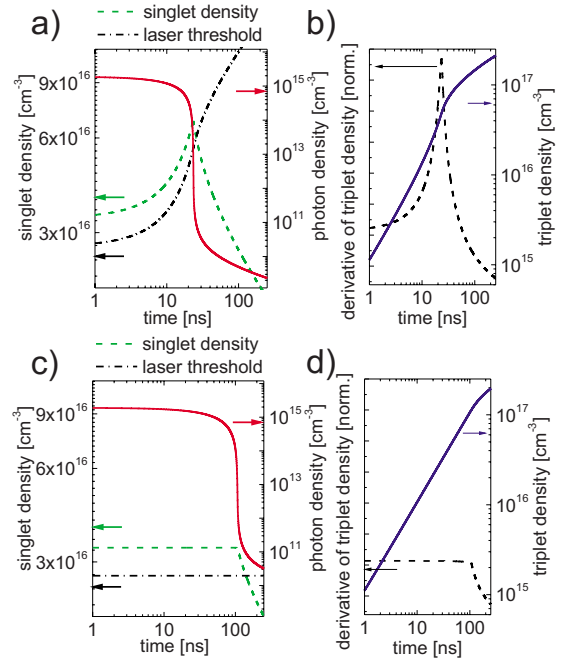


FIG. 5. (Color online) Simulation for ten times the pump intensity as shown in Fig. 4 [(a) and (b)] with and [(c) and (d)] without triplet state absorption.

the generation rate of singlet excitons G). An increased pulse duration from 3 to $\approx 23 \text{ ns}$ can be expected for a pump power density increased by an order of magnitude [Fig. 5(a)]. Without taking the TA into account the lasing duration will increase from 3 to 100 ns, respectively [Fig. 5(c)]. In this regime TA is increasing the laser threshold and therefore increases also the required singlet density to reach threshold. The increasing singlet density accelerates the triplet accumulation [Fig. 5(b)], which further increases the singlet density. Without TA the triplet density is growing only constantly [Fig. 5(d)], which leads to a significantly longer lasing time. Figure 6 shows the ratio of quenched to light emitting singlet excitons. For low excitation near the lasing threshold this ratio is much higher than for a high excitation energy. This is due to the strongly decreasing singlet lifetime above the lasing threshold. As we have shown above, TA cannot be neglected for longer excitation pulses and at higher excitation

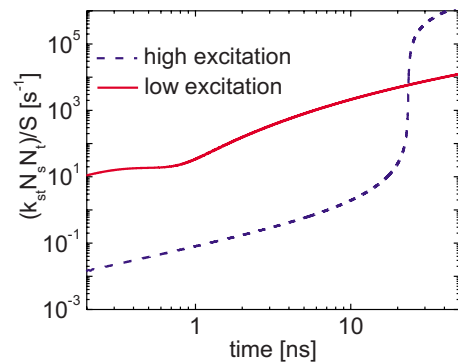


FIG. 6. (Color online) Comparison of the ratio between light emitting and quenched singlet excitons for an excitation energy 12% above lasing threshold and an energy density ten times higher.

densities. In these regimes the duration of the laser output is substantially shortened. For short pulse excitation with an excitation energy near to the lasing threshold, as it is the case in most diode pumped OSLs, triplets cannot accumulate to a level where TA has a major influence. Here TSA is the dominant effect, as we have shown in Fig. 4. A very important message from our model is that TA cannot be neglected for excitation pulses of more than several ns. Giebink and Forrest⁶ studied OSL pumped with a 200 ns pump pulse and reached triplet densities on the order of 10^{17} cm⁻³. Assuming an TA cross section of 10^{-16} cm², as reported for many materials, at the lasing wavelength TA must be considered. Reufer *et al.*⁷ observed an increasing triplet density above the lasing threshold. This observation is easily explained by our model and can be directly seen in Figs. 4 and 5.

IV. SUMMARY

In conclusion we have studied the dynamics of a diode pumped organic semiconductor laser. With highly sensitive,

independent experiments we determined reliable data for the gain cross section, triplet-singlet annihilation, and triplet state absorption in the organic gain medium used for the laser. Based on this input data, the laser dynamics have been favorably modeled with rate equations. Based on these results, we have shown that both effects triplet state absorption and triplet singlet annihilation are indispensable to fully explain the dynamics of organic solid-state lasers. Especially at higher excitation densities absorption due to piled-up triplet excitons (in form of elevated waveguide absorption) cause a termination of lasing within a few nanoseconds.

ACKNOWLEDGMENT

We gratefully acknowledge financial support by the German Federal Ministry for Education and Research BMBF (Grant No. FKZ 13N8166A).

*t.riedl@uni-wuppertal.de

¹D. Schneider, S. Hartmann, T. Benstem, T. Dobbertin, D. Heithecker, D. Metzendorf, E. Becker, T. Riedl, H. H. Johannes, W. Kowalsky, T. Weimann, P. Hinze, and J. Wang, *Appl. Phys. B: Lasers Opt.* **77**, 399 (2003).

²T. Riedl, T. Rabe, H. H. Johannes, W. Kowalsky, J. Wang, T. Weimann, P. Hinze, B. Nehls, T. Farrell, and U. Scherf, *Appl. Phys. Lett.* **88**, 241116 (2006).

³J. M. Lupton, *Nature (London)* **453**, 459 (2008).

⁴O. G. Peterson, S. A. Tuccio, and B. B. Snaveley, *Appl. Phys. Lett.* **17**, 245 (1970).

⁵T. Rabe, K. Gerlach, T. Riedl, H. Johannes, W. Kowalsky, J. Niederhofer, W. Gries, J. Wang, T. Weimann, P. Hinze, F. Galbrecht, and U. Scherf, *Appl. Phys. Lett.* **89**, 081115 (2006).

⁶N. C. Giebink and S. R. Forrest, *Phys. Rev. B* **79**, 073302 (2009).

⁷M. Reufer, J. M. Lupton, and U. Scherf, *Appl. Phys. Lett.* **89**, 141111 (2006).

⁸K. L. Shaklee and R. F. Leheny, *Appl. Phys. Lett.* **18**, 475 (1971).

⁹T. Rabe, S. Hamwi, J. Meyer, P. Görrn, T. Riedl, H.-H. Johannes, and W. Kowalsky, *Appl. Phys. Lett.* **90**, 151103 (2007).

¹⁰J. M. Winfield, A. Van Vooren, M. Park, D. Hwang, J. Cornil, J. Kim, and R. H. Friend, *J. Chem. Phys.* **131**, 035104 (2009).

¹¹G. Bernardo, A. Charas, L. Alcacer, and J. Morgado, *J. Appl. Phys.* **103**, 084510 (2008).

¹²H. A. Mizes and E. M. Conwell, *Phys. Rev. B* **50**, 11243 (1994).

¹³P. B. Miranda, D. Moses, and A. J. Heeger, *Phys. Rev. B* **64**, 081201(R) (2001).

¹⁴J. W. P. Hsu, M. Yan, T. M. Jedju, L. J. Rothberg, and B. R. Hsieh, *Phys. Rev. B* **49**, 712 (1994).

¹⁵M. Yan, L. J. Rothberg, E. W. Kwock, and T. M. Miller, *Phys. Rev. Lett.* **75**, 1992 (1995).

¹⁶D. Moses, A. Dogariu, and A. J. Heeger, *Phys. Rev. B* **61**, 9373 (2000).

¹⁷N. F. Colaneri, D. D. C. Bradley, R. H. Friend, P. L. Burn, A. B. Holmes, and C. W. Spangler, *Phys. Rev. B* **42**, 11670 (1990).

¹⁸A. Sakamoto, O. Nakamura, G. Yoshimoto, and M. Tasumi, *J. Phys. Chem. A* **104**, 4198 (2000).

¹⁹Y. V. Romanovskii, V. I. Arkhipov, and H. Bässler, *Phys. Rev. B* **64**, 033104 (2001).

²⁰M. Yan, L. J. Rothberg, F. Papadimitrakopoulos, M. E. Galvin, and T. M. Miller, *Phys. Rev. Lett.* **73**, 744 (1994).

²¹J. J. M. Halls, K. Pichler, R. H. Friend, S. C. Moratti, and A. B. Holmes, *Appl. Phys. Lett.* **68**, 3120 (1996).

²²W. E. Moerner and S. M. Silence, *Chem. Rev.* **94**, 127 (1994).

²³C.-L. Lee, X. Yang, and N. C. Greenham, *Phys. Rev. B* **76**, 245201 (2007).

²⁴A. P. Monkman, H. D. Burrows, M. da G. Miguel, I. Hamblett, and S. Navaratnam, *Chem. Phys. Lett.* **307**, 303 (1999).

²⁵G. D. Hale, S. J. Oldenburg, and N. J. Halas, *Phys. Rev. B* **55**, R16069 (1997).

²⁶J. Yu, R. Lammi, A. J. Gesquiere, and P. F. Barbara, *J. Phys. Chem. B* **109**, 10025 (2005).

²⁷E. J. W. List, U. Scherf, K. Müllen, W. Graupner, C. H. Kim, and J. Shinar, *Phys. Rev. B* **66**, 235203 (2002).

²⁸J. Hofkens, M. Cotlet, T. Vosch, P. Tinnefeld, K. D. Weston, C. Ego, A. Grimsdale, K. Müllen, D. Beljonne, J. L. Bredas, S. Jordens, G. Schweitzer, M. Sauer, and F. De Schryver, *Proc. Natl. Acad. Sci. U.S.A.* **100**, 13146 (2003).

²⁹J. B. Birks, *Photophysics of Aromatic Molecules* (Wiley-Interscience, London, 1970).

³⁰F. Schindler, J. Lupton, J. Feldmann, and U. Scherf, *Adv. Mater.* **16**, 653 (2004).

³¹M. A. Baldo, D. F. O'Brien, M. E. Thompson, and S. R. Forrest, *Phys. Rev. B* **60**, 14422 (1999).

³²C. Gärtner, C. Karnutsch, U. Lemmer, and C. Pflumm, *J. Appl. Phys.* **101**, 023107 (2007).

³³L. P. Candeias, G. Padmanaban, and S. Ramakrishnan, *Chem. Phys. Lett.* **349**, 394 (2001).

³⁴L. Smilowitz, A. Hays, A. Heeger, G. Wang, and J. Bowers, *Synth. Met.* **55**, 249 (1993).

³⁵H. D. Burrows, J. S. de Melo, C. Serpa, L. G. Arnaut, A. P. Monkman, I. Hamblett, and S. Navaratnam, *J. Chem. Phys.* **115**, 9601 (2001).

³⁶Y. Zaushitsyn, K. G. Jespersen, L. Valkunas, V. Sundstrom, and A. Yartsev, *Phys. Rev. B* **75**, 195201 (2007).